

Reduction of electron channeling in EDS using precession

Yifeng Liao*, Laurence D. Marks

Department of Materials Science and Engineering, Northwestern University, Evanston, IL 60208, United States

ARTICLE INFO

Article history:

Received 28 September 2012

Received in revised form

14 November 2012

Accepted 16 November 2012

Available online 23 November 2012

Keywords:

EDS

Precession electron diffraction

Electron channeling

ABSTRACT

We demonstrated that EDS measurement can be significantly improved by precessing the electron beam, thereby reducing electron channeling effects. For a SrTiO₃ specimen orientated along the [001] zone axis, the measured strontium to titanium atomic ratio was 0.74–0.80 using conventional EDS methods, and the ratio was improved to ~0.99 by precessing the electron beam for angles greater than 22.54 mRad. In ALCHEMI-like experiments in which the specimen was tilted to near two-beam condition, the strontium to titanium ratio was insensitive to the deviation from the Bragg condition using a precessed electron beam. Similar reduction of electron channeling effects was also observed in precession-assisted EDS measurements for an L2₁-ordered Fe₂MnAl intermetallic alloy tilted to the [011] zone axis as well as near two-beam conditions.

© 2012 Elsevier B.V. All rights reserved.

1. Introduction

Owing to its superior spatial and energy resolution, analytical transmission electron microscopy (TEM) techniques such as energy dispersive spectroscopy (EDS) and electron energy loss spectroscopy (EELS) have become powerful tools for probing the local chemistry of thin films and nanomaterials. By counting the characteristic X-ray, EDS is capable of measuring heavy elements as accurate as 1–2% in well-structured experiments [1].

However, EDS measurements can be influenced by many factors such as foil thickness, atomic number, and orientation. When electrons travel through a crystal oriented such that dynamical diffraction effects are strong, the Bloch waves can be enhanced on certain atomic planes [2–4]. This can be exploited to probe the local chemistry and site occupation in ordered intermetallics and oxides [5,6], a technique known as atom location by channeling enhanced microanalysis (ALCHEMI) [7]. By setting different deviation parameters s_z from an exact superlattice two-beam condition, the interaction of the electron with particular atomic planes will be changed, leading to a change in EDS and EELS signal intensity [8].

Electron channeling, however, should be avoided in most conventional EDS experiments. The channeling effect is pronounced when diffracted beams are strongly activated, such as at zone-axis or two-beam conditions. This means that the crystal has to be oriented along either a high-index zone axis or at least tilted off a major zone axis in order to minimize the electron channeling, which is inconvenient in practice. For instance, one

wants the specimen to be oriented along a low-index zone axis for high-resolution TEM (HREM), and the most useful diffraction data is typically at or near a zone-axis. When probing nanomaterials, it is often impossible to have all the grains oriented to a high-index zone axis.

Precession electron diffraction (PED), which features a conically-rocking electron beam, has become an alternative method to obtain high quality diffraction data by tilting the beam, rather than the crystal. Invented by Vincent and Midgley [9], PED rocks the beam by deflecting the incident beam twice using the upper scanning coils, then descanning by bottom scanning coils to form a fixed diffraction pattern. It has been shown that a PED pattern is close to what is predicted by the kinematical diffraction theory [10–13]. While it is not correct to interpret PED intensities as kinematical, it appears to be generally true that they are pseudo-kinematical with large structure factors leading to larger experimental intensities, what has been called intensity-ordering [14]. More details about PED structure analysis can be found in references [10–13,15–32]. Whether PED can be combined with other TEM methods has not yet been fully explored, except a recent paper by Estradé et al. who reported enhanced EELS of strontium titanate (SrTiO₃) using PED [33]. In this study, we examine the application of a precessed electron beam in EDS focusing on the local chemical composition.

2. Experimental

An approximately 100 nm thick foil of commercial (001)-oriented SrTiO₃ single crystal was prepared using conventional ion beam milling. The foil was examined in a JEOL 2100F field emission TEM equipped with EDS and EELS systems; the accelerating voltage

* Corresponding author.

E-mail address: Yifeng.Liao@gmail.com (Y. Liao).

was 200 kV. The electron beam was precessed using a home-built precession unit [34,35]. The electron microscope and the precession system were aligned using the method introduced elsewhere [36,37] to ensure that the spectra were obtained from the same region.

The specimen was tilted to a [001] zone axis for the zone-axis EDS measurements. A number of precession angles ranging from 0 to 33.92 mRad were examined. In the ALCHEMI-like experiments, the specimen was tilted to near two-beam conditions ($g=(200)$) with different deviation parameter s_z ; the superlattice diffraction $g=(100)$ was also activated. For each angle, an EDS spectrum without PED was collected as a reference. In addition to SrTiO_3 , an $\text{L}2_1$ -ordered intermetallic alloy with nominal composition of $\text{Fe}_{55}\text{Mn}_{19}\text{Al}_{26}$ (in atomic percent) [38] was examined. The specimen was electropolished to ~ 100 nm [39], and was tilted to different diffraction conditions including the [011] zone axis and near two-beam conditions with $g=(200)$ activated for ALCHEMI-like experiments.

As an independent test of the calibration of the computer attached to the EDS system, the ratio of Sr/Ti reported was measured three times tilted off a zone axis, which gave a result of 0.996 ± 0.04 . This is so close enough to unity that no further corrections of the results are used here; of course this is not always safe. Similarly, the composition of the intermetallic alloy was determined to be $\text{Fe}_{58.8} \pm 1.7\text{Mn}_{15.3} \pm 0.2\text{Al}_{26.6} \pm 1.4$ at off-zone conditions.

3. Results

Fig. 1a shows the Sr/Ti atomic ratio when the thin foil was oriented along the [001] zone axis. A series of precession angles were examined and compared to the corresponding non-PED

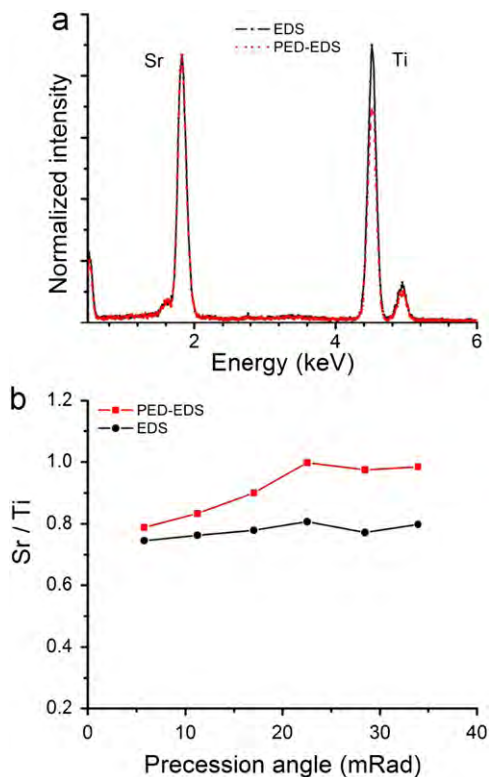


Fig. 1. (a) EDS spectra of SrTiO_3 at the [001] zone axis normalized to the strontium peak. The Ti peak intensity reduced for PED-EDS. The precession angle was set to 33.92 mRad. (b) Sr to Ti ratio as a function of precession angle. The SrTiO_3 single crystal was oriented along the [001] zone axis.

results. In all non-PED EDS tests, the Sr/Ti was in the range 0.75–0.80 with slight fluctuation. In PED-EDS, a small precession angle of 5 mRad led to a Sr/Ti ratio of 0.79, which is insignificantly different from the non-PED results. However, the Sr/Ti ratio increased remarkably with increasing the precession angle, until it reached a plateau of ~ 0.99 when the precession angle was increased to 22.54 mRad. This ratio was insensitive to the precession angle for the angles greater than 22.54 mRad. It is apparent that the electron channeling can be significantly reduced in PED-EDS with a large precession angle, and becomes negligible when the angle is greater than 22.54 mRad at 200 kV for SrTiO_3 . The absolute intensities of the strontium signal decreased slightly with PED; a reduction of 20.0% was observed when the precession angle was set to 33.92 mRad.

EDS spectra were subsequently collected under near two-beam conditions with $s_z < 0$, $s_z = 0$ and $s_z > 0$. The precession angles were set to 22.54 and 47.48 mRad for the ALCHEMI-like measurements. **Fig. 2** shows the Sr/Ti ratio as a function of s_z . For non-PED EDS measurements, the Sr/Ti ratio changed remarkably when s_z changed from negative to positive, as expected in an ALCHEMI experiment. For precession angle of 22.54 mRad, the Sr/Ti ratio was measured to be 0.93 when $s_z = -1.14 \text{ nm}^{-1}$; while for $s_z = 1.34$, this value increased to 1.20. In contrast, in PED-assisted EDS measurements, the Sr/Ti ratio was less sensitive to s_z . The Sr/Ti ratios were measured to be 1.12–1.17 when the precession angle was 22.54 mRad, suggesting that the channeling effects still significantly influenced the results. With increasing the precession angle to 47.48 mRad, the greatest angle that the system can achieve without significantly changing the alignment, the Sr/Ti ratio reduced to ~ 1.04 . Although the electron channeling was not completely eliminated, it is clear that the channeling effects were remarkably suppressed at a larger precession angle.

It is worth noting that the critical angle of 22.54 mRad was obtained for SrTiO_3 at the [001] zone axis in this study. Estradé et al. showed that the enhancement of EELS signal could be saturated for an angle of 8.7 mRad (0.5°) [33], which is much lower than the critical value measured in this study. This value appeared to be also dependent on other factors such as foil thickness and diffraction conditions, rather than material species alone. The oxygen signal still showed a large error in the PED-EDS, suggesting that PED does not improve the capability of measuring light elements (as expected).

As a second confirmation, the composition of the $\text{L}2_1$ -ordered Fe–Mn–Al alloy was examined using both PED-EDS and EDS. The composition measured using EDS at the [011] zone axis was $\text{Fe}_{55.0}\text{Mn}_{14.3}\text{Al}_{30.7}$ with a lower Fe concentration compared to that measured at off-zone-axis conditions ($\text{Fe}_{58.8} \pm 1.7\text{Mn}_{15.3} \pm 0.2\text{Al}_{26.6} \pm 1.4$). In contrast, the composition ($\text{Fe}_{58.3}\text{Mn}_{15.4}\text{Al}_{26.3}$) measured using

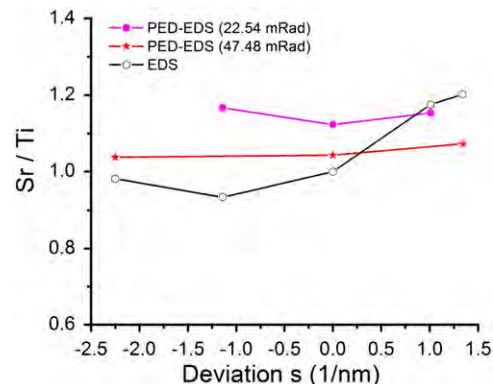


Fig. 2. Sr to Ti ratio as a function of deviation from the two-beam condition. The precession angles were 22.54 and 47.48 mRad.

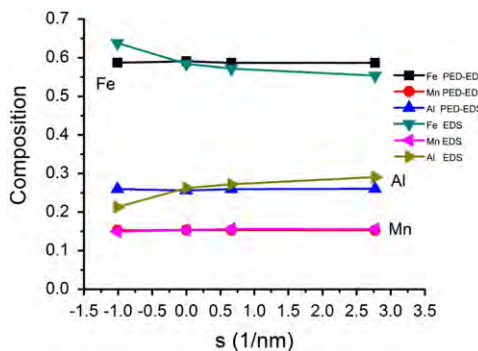


Fig. 3. EDS and PED-EDS measurements of the Fe–Mn–Al alloy as a function of deviation from the two-beam condition. A superlattice reflection $g=(200)$ was activated. The precession angle was set to 47.48 mRad.

PED-EDS with a precession angle of 47.48 mRad is close to the off-zone-axis measurement. Fig. 3 shows the compositions as a function of deviation from $g=(200)$ two-beam condition. The Fe composition determined using conventional EDS varied from ~55% to ~63%, while it remained ~58% for all PED-EDS measurements, indicating that PED is also effective in reducing electron channeling effects for intermetallics.

4. Discussion

The results and their consequences are moderately self-evident. There are clear advantages of using standard techniques which work well on the zone-axis such as HREM, Z-contrast and CBED then switching on precession to obtain accurate EDS measurements. At the same time one can of course obtain a good PED pattern, which for most structures is much more useful than a conventional diffraction pattern.

Two additional points merit mention. First, the removal of channeling effects with PED for EDS for a zone axis orientation as well as the less effective removal under two-beam conditions are strong constraints on simplified explanations of the technique. It strongly suggests that classical expansions for zone-axes orientations in terms of the Bloch waves or a real-space tight-binding model as in channeling while not wrong, are not going to be the clean approach. The results at a two-beam orientation suggest that a systematic-row approximation is more appropriate, as has been suggested in a number of papers dating back to the systematic-row corrections of the Blackman formula. However, this is not everything and it is certain that the averaging over angle for the integrated intensities is also important. A simple explanation of how PED works remains to be determined, and has been somewhat mysterious for a few years.

Secondly, it follows that coupling precession with EELS will in a sense also reduce channeling effects, but one needs to be more cautious. With EDS the signal is implicitly integrated over all scattering angles, but with EELS the geometry of the detection will enter into the results. As is well known, going to large collection angles has drastic effects on EELS spectra so it is not clear that it will be that useful. As mentioned earlier, it has been pointed out that on a zone axis one can get signal-enhanced EELS with precession [33]. However, in a few preliminary experiments we have found that this is not always true if one tilts off the zone axis.

5. Conclusions

We have demonstrated that PED significantly reduces electron channeling effects under strong diffraction conditions such as

zone axis and two-beam conditions. The EDS measurement can be significantly improved with PED. For the [001] zone axis, the Sr/Ti ratio measured using EDS was consistently ~0.99 when the precession angle greater than 22.54 mRad. For ALCHEMI-like experiments, the channeling effects were largely suppressed when at a higher angle of 47.48 mRad. The reduction of electron channeling effects was also demonstrated for the L2₁-ordered Fe–Mn–Al intermetallic alloy. The compositions measured using PED-EDS were insensitive to the diffraction condition and were consistent with the off-zone-axis EDS measurement.

Acknowledgments

This research is supported by the NSF on Grant number CMMI-1030703 and by the NIH on Grant number 1RC2AR058993-01. The authors are indebted to Professor Ian Baker at Dartmouth College, Mr. Yuyuan Lin, and Dr. Houari Amari for helpful discussions and for providing the specimens.

References

- [1] H. Amari, M.J. Kappers, C.J. Humphreys, C. Cheze, T. Walther, Measurement of the Al content in AlGaN epitaxial layers by combined energy-dispersive X-ray and electron energy-loss spectroscopy in a transmission electron microscope, *Physica Status Solidi C* 9 (2012) 1079–1082.
- [2] P. Duncumb, Enhanced X-ray emission from extinction contours in a single-crystal gold film, *Philosophical Magazine* 7 (1962) 2101.
- [3] P.B. Hirsch, M.J. Whelan, A. Howie, On production of x-rays in thin metal foils, *Philosophical Magazine* 7 (1962) 2095.
- [4] J. Tafto, Electron channeling, structure factor phases, polarity and atom site determination in crystals, *Micron* 34 (2003) 157–166.
- [5] Z.H. Zhang, X.F. Wang, J.B. Xu, S. Muller, C. Ronning, Q. Li, Evidence of intrinsic ferromagnetism in individual dilute magnetic semiconducting nanostructures, *Nature Nanotechnology* 4 (2009) 523–527.
- [6] Y.Z. Liu, Q.Y. Xu, H. Schmidt, L. Hartmann, H. Hochmuth, M. Lorenz, M. Grundmann, X.D. Han, Z. Zhang, Co location and valence state determination in ferromagnetic ZnO: Co thin films by atom-location-by-channeling-enhanced-microanalysis electron energy-loss spectroscopy, *Applied Physics Letters* 90 (2007) 154101–154103.
- [7] J.C.H. Spence, J. Tafto, ALCHEMI—a new technique for locating atoms in small crystals, *Journal of Microscopy*—Oxford 130 (1983) 147–154.
- [8] J. Tafto, G. Lehmkuhl, Direction dependence in electron-energy loss spectroscopy from single-crystals, *Ultramicroscopy* 7 (1982) 287–294.
- [9] R. Vincent, P.A. Midgley, Double conical beam-rocking system for measurement of integrated electron diffraction intensities, *Ultramicroscopy* 53 (1994) 271–282.
- [10] K. Gjonne, On the integration of electron diffraction intensities in the Vincent–Midgley precession technique, *Ultramicroscopy* 69 (1997) 1–11.
- [11] K. Gjonne, Y.F. Cheng, B.S. Berg, V. Hansen, Corrections for multiple scattering in integrated electron diffraction intensities. Application to determination of structure factors in the [001] projection of AlmFe, *Acta Crystallographica Section A* 54 (1998) 102–119.
- [12] S.S. Brown, I.C. Clarke, A review of lubrication conditions for wear simulation in artificial hip replacements, *Tribology and Lubrication Technology* 62 (2006) 54–61.
- [13] P. Oleynikov, S. Hovmoller, X.D. Zou, Precession electron diffraction: observed and calculated intensities, *Ultramicroscopy* 107 (2007) 523–533.
- [14] L.D. Marks, W. Sinkler, Sufficient conditions for direct methods with swift electrons, *Microscopy and Microanalysis* 9 (2003) 399–410.
- [15] W. Sinkler, C.S. Own, L.D. Marks, Application of a 2-beam model for improving the structure factors from precession electron diffraction intensities, *Ultramicroscopy* 107 (2007) 543–550.
- [16] J. Ciston, B. Deng, L.D. Marks, C.S. Own, W. Sinkler, A quantitative analysis of the cone-angle dependence in precession electron diffraction, *Ultramicroscopy* 108 (2008) 514–522.
- [17] B.S. Berg, V. Hansen, P.A. Midgley, J. Gjonne, Measurement of three-dimensional intensity data in electron diffraction by the precession technique, *Ultramicroscopy* 74 (1998) 147–157.
- [18] J. Gjonne, V. Hansen, A. Kverneland, The precession technique in electron diffraction and its application to structure determination of nano-size precipitates in alloys, *Microscopy and Microanalysis* 10 (2004) 16–20.
- [19] W. Sinkler, L.D. Marks, Characteristics of precession electron diffraction intensities from dynamical simulations, *Zeitschrift Fur Kristallographie* 225 (2010) 47–55.
- [20] E.F. Rauch, J. Portillo, S. Nicolopoulos, D. Bultreys, S. Rouvimov, P. Moeck, Automated nanocrystal orientation and phase mapping in the transmission electron microscope on the basis of precession electron diffraction, *Zeitschrift Fur Kristallographie* 225 (2010) 103–109.

- [21] P. Moeck, S. Rouvimov, Precession electron diffraction and its advantages for structural fingerprinting in the transmission electron microscope, *Zeitschrift Fur Kristallographie* 225 (2010) 110–124.
- [22] J. Hadermann, A.M. Abakumov, A.A. Tsirlin, V.P. Filonenko, J. Gonnissen, H.Y. Tan, J. Verbeeck, M. Gemmi, E.V. Antipov, H. Rosner, Direct space structure solution from precession electron diffraction data: resolving heavy and light scatterers in $Pb_{13}Mn_9O_{25}$, *Ultramicroscopy* 110 (2010) 881–890.
- [23] M. Gemmi, H. Klein, A. Rageau, P. Strobel, F. Le Cras, Structure solution of the new titanate $Li_4Ti_8Ni_2O_{21}$ using precession electron diffraction, *Acta Crystallographica Section B—Structural Science* 66 (2010) 60–68.
- [24] W. Sinkler, C.S. Own, J. Ciston, L.D. Marks, Statistical treatment of precession electron diffraction data with principal components analysis, *Microscopy and Microanalysis* 13 (Suppl. 2) (2007) 954CD–955CD, Proceedings.
- [25] J. Gjønnes, V. Hansen, B.S. Berg, P. Runde, Y.F. Cheng, K. Gjønnes, D.L. Dorset, C.J. Gilmore, Structure model for the phase AlmFe derived from three-dimensional electron diffraction intensity data collected by a precession technique. Comparison with convergent-beam diffraction, *Acta Crystallographica Section A* 54 (1998) 306–319.
- [26] C.S. Own, W. Sinkler, L.D. Marks, Rapid structure determination of a metal oxide from pseudo-kinematical electron diffraction data, *Ultramicroscopy* 106 (2006) 114–122.
- [27] A. Kverneland, V. Hansen, R. Vincent, K. Gjønnes, J. Gjønnes, Structure analysis of embedded nano-sized particles by precession electron diffraction. eta η' -precipitate in an Al-Zn-Mg alloy as example, *Ultramicroscopy* 106 (2006) 492–502.
- [28] A. Kverneland, V. Hansen, G. Thorkildsen, H.B. Larsen, P. Pattison, X.Z. Li, J. Gjønnes, Transformations and structures in the Al-Zn-Mg alloy system: a diffraction study using synchrotron radiation and electron precession, *Materials Science and Engineering A—Structural Materials* 528 (2011) 880–887.
- [29] E. Mugnaioli, T. Gorelik, U. Kolb, “Ab initio” structure solution from electron diffraction data obtained by a combination of automated diffraction tomography and precession technique, *Ultramicroscopy* 109 (2009) 758–765.
- [30] C.S. Own, A.K. Subramanian, L.D. Marks, Quantitative analyses of precession diffraction data for a large cell oxide, *Microscopy and Microanalysis* 10 (2004) 96–104.
- [31] P.A. Midgley, M.E. Sleight, M. Saunders, R. Vincent, Measurement of Debye-Waller factors by electron precession, *Ultramicroscopy* 75 (1998) 61–67.
- [32] A. Avilov, K. Kuligin, S. Nicolopoulos, M. Nickolskiy, K. Boulahya, J. Portillo, G. Lepeshov, B. Sobolev, J.P. Collette, N. Martin, A.C. Robins, P. Fischione, Precession technique and electron diffractometry as new tools for crystal structure analysis and chemical bonding determination, *Ultramicroscopy* 107 (2007) 431–444.
- [33] S. Estrade, J. Portillo, L. Yedra, J.M. Rebled, F. Peiro, EELS signal enhancement by means of beam precession in the TEM, *Ultramicroscopy* (2012) 135–137.
- [34] C.S. Own, System Design and Verification of the Precession Electron Diffraction Technique, Department of Materials Science and Engineering, Northwestern, Evanston, 2005 161.
- [35] C.S. Own, L.D. Marks, W. Sinkler, Electron precession: a guide for implementation, *Review of Scientific Instruments* 76 (2005).
- [36] Y.F. Liao, L.D. Marks, On the alignment for precession electron diffraction, *Ultramicroscopy* 117 (2012) 1–6.
- [37] C.T. Koch, Aberration-compensated large-angle rocking-beam electron diffraction, *Ultramicroscopy* 111 (2011) 828–840.
- [38] Y.F. Liao, I. Baker, Study of yield stress anomaly of Fe_2MnAl single crystal by in situ TEM straining, *Philosophical Magazine* 92 (2012) 959–985.
- [39] Y.F. Liao, F.L. Meng, I. Baker, L12 precipitates within L21 ordered $Fe-21.7Mn-14.5Al$, *Philosophical Magazine* 91 (2011) 3547–3556.